Prediction of the Polar Morphology of Sodium Chlorate Using a Surface-Specific Attachment Energy Model

G. Clydesdale, K. J. Roberts,* and G. B. Telfer

Centre for Molecular and Interface Engineering, Department of Mechanical and Chemical Engineering, Heriot-Watt University, Riccarton, Edinburgh EH14 4AS, UK

V. R. Saunders

CCLRC Daresbury Laboratory, Warrington WA4 4AD, UK

D. Pugh

Department of Pure and Applied Chemistry, University of Strathclyde, 295 Cathedral Street, Glasgow G1 1XL, UK

R. A. Jackson

Department of Chemistry, University of Keele, Keele, Staffordshire ST5 5BG, UK

P. Meenan

Experimental Station, E.I. du Pont de Nemours, Wilmington, Delaware 19880-0304

Received: December 8, 1997; In Final Form: May 18, 1998

A morphological prediction of the polar crystal morphology of the molecular ionic solid sodium chlorate is presented. This prediction uses interatomic potential calculations that employ surface-specific attachment energy calculations associated with an ab initio calculation of surface charges via a Hartree−Fock calculation using periodic boundary conditions. The data predicts assignment of the absolute polarity of the crystal with respect to the published crystal structure (Burke-Laing, M. E.; Trueblood, K. N. *Acta Crystallogr.* **1977**, *B33*, 2698), which reveals the chlorate-rich {−1 −1 −1} to be the observed form rather than its sodium-rich Freidel opposite, {111}. The predicted crystal morphology is in reasonable agreement with observed morphologies, although there is an underestimation of the dominant {200} form. The latter is rationalized with experimental data in terms of a face-specific solvent binding model.

Introduction

In recent times the use of molecular, surface, interface, and solid state modeling techniques in defining the processing properties of inorganic particulate solids has become increasingly important. It is widely accepted that morphological simulations based on surface attachment energy calculations[1−7] are considered a more accurate representation than those based on the Bravais-Freidel-Donnay-Harker (BFDH) lattice geometry laws.[8−10] The former technique has been successfully applied to a variety of organic molecular crystals, e.g.[11,12] However, its application has been more limited in the area of molecular ionic systems, such as perchlorates and phosphates,[13,14] because of the hitherto nonavailability of well-defined interatomic potential parameters. These parameters are required to simulate the interactions taking place within the material so that structure and properties may be determined.

Such a potential has recently been developed for alkali chlorates and bromates:[15] the potential parameters are therefore now available to carry out energy calculations on sodium chlorate. There remains, however, the fact that for ionic materials, long-range forces dominate, rendering the calculations involved in the attachment energy process more complex. This difficulty can be addressed by utilizing accelerated convergence techniques. These techniques have allowed us, in the work presented here, to produce morphological models, including the simulation of the polar nature of sodium chlorate, by the use of accurate, surface-specific atomic charges.

Sodium chlorate is used widely in the paper and pulp industry as a source of bleach, and is also used as a herbicide and defoliant in the agricultural industry. The computational studies described here have been carried out to study the problems associated with its recrystallization and filtration, which is directly impacted upon by particulate shape and size.

Crystal Chemistry and Morphology

In the solid-state, sodium chlorate crystallizes in the cubic space group $P2_13$ ($a = 6.575$ Å) with four $NaClO_3$ formula units in the unit cell.[16] Elastic constants determined by Viwanathany in 1966[17] produce an anisotropy factor of 1.51, indicating that the system is moderately isotropic.

The role of external conditions of growth on the formation of crystals of a particular morphology was pointed out by Bunn.[18] When external conditions are fairly uniform for example when crystals are growing in a rapid manner in well-stirred, highly supersaturated solutions (thereby providing a good supply of solute around the crystal), sodium chlorate is known

S1089-5647(98)00456-8 CCC: $15.00
Published on Web 08/14/1998

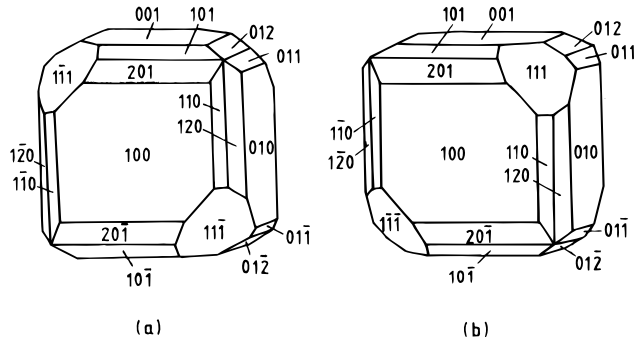

Figure 1. (a) Left- and (b) right-handed experimental morphologies, after Szurgot and Szurgot.[25]

to crystallize as cubes with the {100} form. The converse situation (i.e., low supersaturation, stagnant conditions, and a poor supply of solute) can cause highly faceted crystals with a number of faces rarely observed under stable growth conditions. Wojciechowski[19] found that for sodium chlorate crystals grown at low supersaturations, the theoretical morphology should be cubic with, additionally, four polar {111} type faces and 12 {110} type faces, together with the minor {120} form. This work seems to be in contrast to that of Kern[20] who observed the effect of supersaturation on the morphology of sodium chlorate. According to this work, the form is totally cubic with the tetrahedral faces appearing at higher supersaturations. However, these results were contradicted by Simon[21] who discovered that the only growth form is cubic at high supersaturation, with additional faces appearing as saturation is decreased. Simon also cited the appearance of {110}, {120}, and {111} forms as not only the result of supersaturation itself, but strongly dependent on the direction of solution flow. Thus, it might be that the more complex crystals observed by Simon reflected a more defective and highly strained material. Confirmation for this hypothesis was provided by Hooper et al.[22] who found crystals with a simple cubic habit to be of much higher perfection than those exhibiting a more complex morphology.

It appears that the contradictory problem arises from the following two different aspects concerned in the determination of macromorphology. First, predictions are made on the basis of the crystallographic structure and second, taking into consideration the various growth factors. Confusion of these two concepts can lead to misleading conclusions regarding the actual morphology prepared under practical crystallization conditions. It would seem, however, that whichever is the case, sodium chlorate can exhibit {110}, {120}, and {111} forms as well as the cubic {100}.

Sodium chlorate is known to be optically active with its absolute configuration being first determined by Ramachandran and Chandrasekaran in 1957.[23,24] Very recently, Szurgot and Szurgot[25] studied its enantiomorphic nature. This effect is restricted to the solid state because no optical activity is observed in aqueous solution. This would seem to indicate that the molecular structure itself is not enantiomorphic. Figure 1 shows the left-handed and right-handed crystals of sodium chlorate. The polar nature of the {111} surfaces reflects the packing of the chlorate anions, which are symmetrically aligned with respect to the 3-fold axis of the crystal unit cell. In this cell, the three oxygen atoms are exposed to one of the polar surfaces with the chlorine atoms exposed to the other surface. The assignment of absolute polarity of the overall structure depends on the enantiomeric form of the crystal used for the crystal structure determination, which is not provided in the published structure.[16]

Details of Calculations. *Morphological Simulation Using the Attachment Energy Method.* The attachment energy (E_{att}) is the energy released when a new layer of molecules joins onto the surface of a crystal, and involves the addition of a slice of thickness d_{hkl}, where this is the interplanar spacing. The actual formation of this slice also gives rise to an output of energy. This is classified as the slice energy, E_{sl}. The total lattice energy, E_{cr}, is defined by[1]

$$E_{cr} = E_{sl} + E_{att} \tag{1}$$

Hartman and Bennema[11] have shown that the faces of greater morphological importance in the final form (i.e., those that dominate the crystal habit) arise from the smaller values of attachment energy, that is, the growth rate of a face is proportional to E_{att}. Derivations using this method are called "growth morphologies" and can be calculated using computer programs. For this work, calculations of the lattice, slice, and attachment energies were carried out using the program HABIT98, a development version of HABIT95 that is outlined later and described in detail elsewhere.[26] Morphological visualization was carried out using Cerius[2] molecular modeling software.[27]

The parameter E_{cr} is calculated by summing all nonbonded atom−atom interactions from a central molecule or ion within a three-dimensional(3-D) model of the crystal, generated from the structural data.[28] However, calculations on inorganic systems, using this method, in previous studies[29] proved unsuccessful because of the slow convergence of the lattice energy, causing the summation to extend beyond reasonable computational limits. This result can be explained by considering eq 2, which shows the interaction energy (V) between two atoms, i and j, separated by a distance, r. The first two terms in the equation represent van der Waals attraction and repulsion. Organic materials are generally dominated by these forces, which depend on r^{-6} and r^{-12} and therefore fall off sharply with distance. In contrast, inorganic materials are dominated by the longer range electrostatic forces (the third term in eq 2), which converge slowly.

$$V_{ij} = -A/r_{ij}^{\ 6} + B/r_{ij}^{\ 12} + q_i q_j / r_{ij} \tag{2}$$

To aid convergence for the ionic material used in this study, Evjen's method[30] in three dimensions was implemented in a development version of HABIT95. This method involves setting up neutral 3-D regions around the central cell, with charges at the edges and surfaces shared out. Figure 2 demonstrates how the lattice energy is more quickly convergent using this technique. The intermolecular interactions were calculated using the potential parameters developed for chlorates by Telfer et al.[15] (see Table 1). This potential includes values for charges derived alongside the force field, so both van der Waals and Coulombic contributions are considered.

The employment of Evjen's method also allowed the calculation of more realistic attachment energies. To calculate these, E_{cr} was partitioned between E_{sl} and E_{att}, as in eq 1. To allow for slices that can be defined in more than one way, the position of the growth slice was adjusted within the crystal structure (the slice is illustrated in Figure 3). To aid in the selection of the most stable slice (lowest slice energy) per face, E_{sl} was calculated for a sequence of slices.[26] The slice boundaries were moved along the growth normal (keeping d_{hkl} constant) by 20

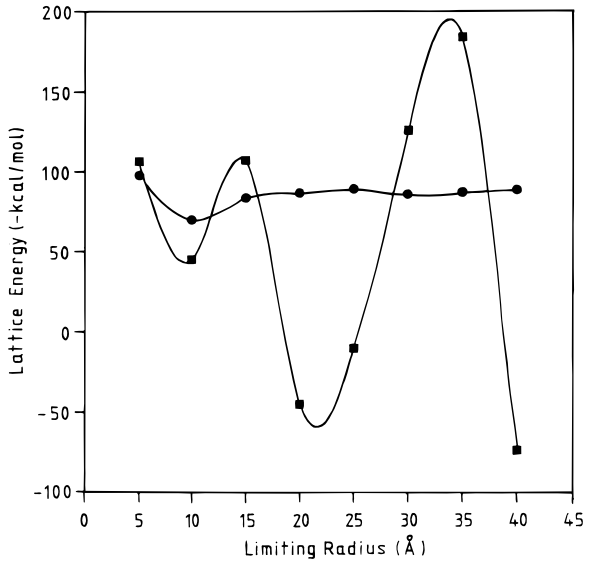

Figure 2. Relationship between lattice energy and summation distance for sodium chlorate before (■) and after (●) the Evjen method[30] is employed, showing how this improves convergence.

TABLE 1: Short-Range Potential Parameters for Sodium Chlorate[a]

interaction	*A*, eV	*ρ*, Å
Na−O	645.733	0.2973
Cl−O	893.286	0.3088
O−O	22764.300	0.1490

[a] C (eVÅ^6) = 0 for cation−oxygen interaction and 30.273 for O−O interaction. Charges (|*e*|): *q*(Na) = 1.0; *q*(Cl) = 0.927, and *q*(O) = −0.642.

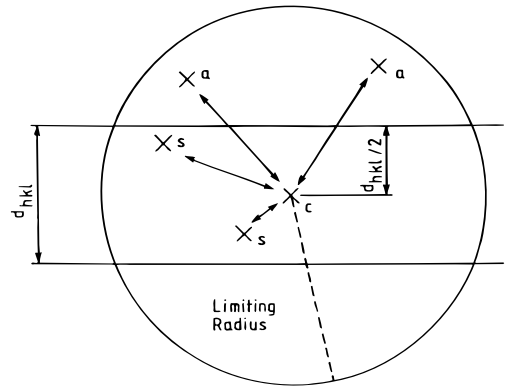

Figure 3. Basic approach for calculating the intermolecular interactions using the atom−atom method, showing how the lattice energy can be partitioned between the slice and attachment energies within a limiting sphere: X_c is the central molecule, X_a is a molecule outside the slice, and X_s is a molecule inside the slice. Note that the slice boundaries defined by d_{hkl} may be shifted along the growth normal to obtain the most energetically favorable slice.

equal steps from $-d_{hkl}/2$ to $+d_{hkl}/2$, with the center of the slice unmoved, until the surface structure was repeated. For each step E_{sl} was calculated; however, E_{sl} is not calculated at the limiting shifts of $d_{hkl}/2$, as here the slice center cuts the surface. Figure 4 shows a plot of slice energy against slice number, from which can be ascertained the most stable slice for each growth face of sodium chlorate. The step chosen was that with the most negative E_{sl} value, and for steps which gave identical E_{sl} values, the closest to the slice center was used. The E_{att} value associated with the most stable slice was calculated directly. From a list of E_{att} faces for likely growth faces, morphological models were predicted.

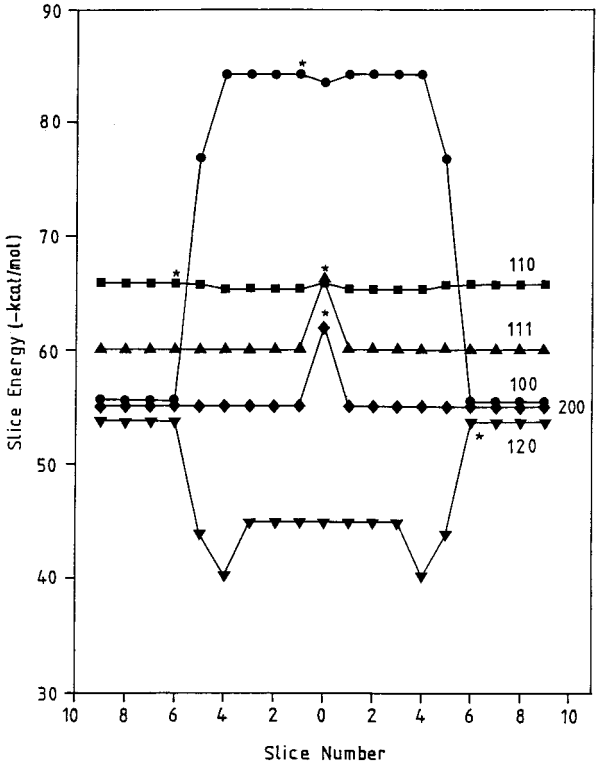

Figure 4. Plot of slice energy versus slice step number showing the most stable slice for each habit face.

Simulation of the Polar Nature of Sodium Chlorate. One area that has seldom been investigated using theoretical methodologies (see, however, refs 31 and 32) relates to crystals that exist in noncentrosymmetric space groups and possess directions of a polar nature. This polarity of structure can, in turn, lead to the development of a polar morphology. Here, although two surfaces are related by symmetry, they can grow at very different rates, leading to unequal development of (*hkl*) and (−*h* −*k* −*l*) faces. Kinetic factors such as unequal solvent binding to the polar faces are often assumed to be the cause of these differences. Indeed, this case has been shown for resorcinol growing from aqueous solution.[33] Any lack of theoretical development in this area has been mainly because the predictive models utilized considered the calculation of attachment energies between stoichiometric slices in crystal systems. By definition, these calculations assume a center of symmetry and so $E_{att}(hkl)$ is always equal to $E_{att}(-h\ -k\ -l)$ because the Coulombic part of the intermolecular potential function in the bulk solid state contains no surface-specific interaction parameters.[32] This equality is demonstrated in Figure 5. The simulation of the polarity of a crystal from a structural perspective requires the calculation of highly accurate partial atomic charges on each face, thus allowing the intermolecular bond strengths involving atoms at the polar surfaces to differ. This, in turn, allows the production of unequal E_{att} values. Very small changes in the attachment energy can have a much greater effect on the predicted morphology.

The polar morphology of sodium chlorate was simulated by calculating the surface atomic charges of all likely growth faces using the quantum mechanical program CRYSTAL92.[34] This program allows wave functions and properties of crystalline systems to be calculated (see, for example, refs 35−37) using a Hartree−Fock Linear Combination of Atomic Orbitals (HF-LCAO) approximation, giving an understanding of how molecular polarization is influenced by the crystal field.[38,39] Calculations were also carried out to determine the atomic

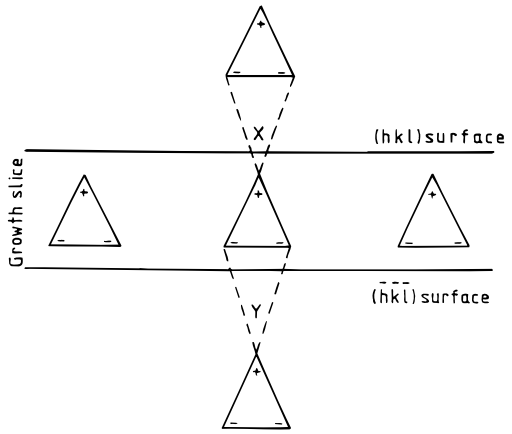

Figure 5. Schematic diagram showing how the classical attachment energy model, based on the bulk solid-state structure, does not allow the prediction of polar effects because the intermolecular bonds (marked X) formed on attachment to the (*hkl*) face are identical to those marked Y on the $(-h\ -k\ -l)$ face.[32]

charges in the crystal bulk using a complete unit cell, and for an isolated sodium chlorate ion pair.

Using the results from these calculations, attachment energies were obtained from the polar morphology calculation mode of HABIT98. The overall computational procedure used here is very similar to that of a classical attachment energy calculation, except that atoms on the surface are assigned different electronic charges from atoms in the bulk, simulating the effects due to surface polarity. However, because the potential parameters used possess their own charge distribution, the surface and isolated charges calculated via the quantum chemical study were scaled in accordance with those. This scaling was also carried out with respect to the charges for the bulk calculation, because the potential model was based on that of a bulk crystal. It should be noted that the rest of the potential was not rescaled to each surface, despite the fact that the surface charges differ from those in the bulk. However, it was assumed that the Coulombic part of the potential will be most sensitive to surface effects, and the approximation has been made that the rest of the potential remains the same as that in the bulk.

Results and Discussion

Lattice Energy Calculations. The calculated lattice energy for sodium chlorate was -177.28 kcal mol^{-1}, which compares well with the value of -184.03 kcal mol^{-1} obtained from a Born-Fajans-Haber cycle.[40] Table 2 lists the van der Waals and electrostatic contributions for the strongest calculated intermolecular interactions. It can be noted that the number of dominant interaction types exceeds that found in a typical organic system, where the Coulombic contribution is small. Within the organic system, this result means that the total energy of the individual interactions will decrease more rapidly as the attractive and repulsive forces tend toward equalling out and the electrostatic portion begins to exert very little effect. This relationship is not the case in an ionic system where the Coulombic forces contribute to the overall energy at much greater distances.

Classical Attachment Energy Morphological Simulation. A BFDH analysis of sodium chlorate was carried out to identify the faces likely to dominate the crystal morphology, based on their interplanar spacings; these were {110}, {111}, {200}, and {120}. The attachment energies of these growth forms were calculated (the results are given in Table 3, column 2), thus producing the theoretical morphology shown in Figure 6a. The experimentally obtained morphology is shown in Figure 1.[25]

TABLE 2: Individual Contributions for the Calculated Anion−Cation Bonds in Sodium Chlorate[a]

distance, Å	position $[UVWZ]_i-[UVWZ]_j$	attractive energy	replusive energy	Coulombic energy	total energy
3.29	[0001]−[−1014]	0.00	2.27	−56.76	−54.40
3.48	[0001]−[−1004]	0.00	1.68	−45.59	−43.91
4.31	[0001]−[0001]	0.00	0.00	−28.74	−28.74
5.39	[0001]−[0011]	0.00	0.00	−30.92	−30.92
6.29	[0002]−[1102]	0.00	0.00	−28.33	−28.33
6.60	[0002]−[0−111]	0.00	0.00	−24.79	−24.79
6.69	[0002]−[0011]	0.00	0.00	−22.14	−22.14
7.08	[0002]−[−1−112]	0.00	0.00	−25.03	−25.03
7.27	[0001]−[1102]	0.00	0.00	−24.40	−24.40
7.35	[0003]−[00−11]	0.00	0.00	−23.44	−23.44

[a] Bonds are between pairs of ions *i* and *j* in asymmetric units identified by [UVWZ], where U, V, and W are multiples of the lattice constants a, b, and c; *Z* is the symmetry position of the asymmetric unit within the unit cell ($Z = 1$ is x, y, z; $Z = 2$ is $-x + 1/2, -y, z + 1/2$; $Z = 3$ is $-x, y + 1/2, -z + 1/2$; $Z = 4$ is $x + 1/2, -y + 1/2, -z$); energy values are in kcal mol^{-1}.

TABLE 3: Attachment Energy Values (in kcal mol^{-1}) for Classical and Polar Morphology Models[a]

face (*h k l*)	classical model	bulk/isolated model	surface/isolated model
110	−22.78 (0.878)	−22.32 (0.896)	−20.00 (1.000)
111	−22.40 (0.893)	−22.22 (0.900)	−23.81 (0.840)
−1 −1 −1	−22.40 (0.893)	−22.22 (0.900)	−20.08 (0.996)
200	−26.63 (0.751)	−26.11 (0.766)	−26.70 (0.749)
120	−34.88 (0.573)	−33.94 (0.589)	−24.42 (0.819)

[a] To allow easier comparison, values in parentheses are normalized to the (110) face for the surface/isolated model.

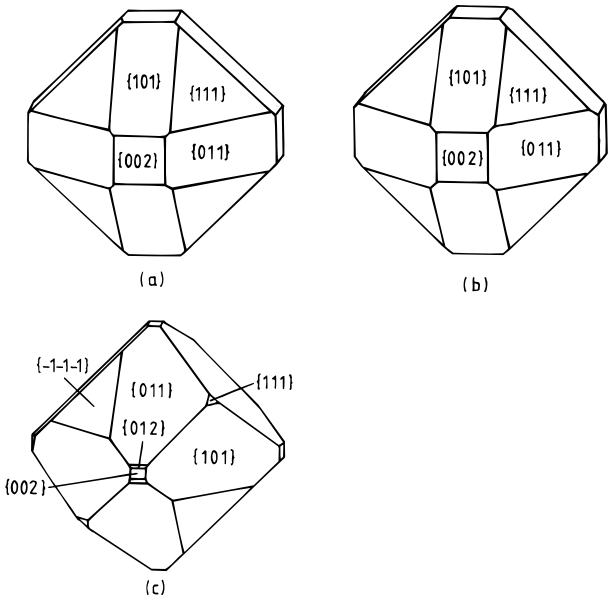

Figure 6. Morphologies of sodium chlorate: (a) theoretical morphology obtained using attachment energy method with Evjen modification and parameters from ref 15; (b) polar simulation using bulk/isolated charge set; (c) polar simulation using surface/isolated charge set.

The form of the morphology is basically that of a cube, with dominant {200} and smaller tetrahedral {111} forms and {110}. Less commonly, the appearance of very small {120} forms have been noted. Overall, the forms of the experimental crystal are reproduced by the simulation, however the {200} form tends to be underestimated. In addition, the {111} and {−1 −1 −1} faces have the same relative growth rates, as would be expected

TABLE 4: Atomic Charges (in electron units) Used in Polar Morphology Predictions[a]

atom (x, y, z)	bulk unscaled	bulk	isolated	(110) surface	(111) surface	(−1 −1 −1) surface	(200) surface	(120) surface
Na (0.0683, 0.0683, 0.0683)	0.983	1.000	0.998	0.988	0.979	1.002	0.997	0.995
							0.995	
Cl (0.4182, 0.4182, 0.4182)	1.451	0.927	0.879	0.912	0.889	0.914	0.903	0.893
				0.937	0.889	0.914	0.922	
					0.889	0.914		
					1.001	0.906		
O1 (0.3034, 0.5931, 0.5053)	−0.811	−0.642	−0.696	−0.677	−0.691	−0.705	−0.649	−0.581
				−0.618	−0.536	−0.475	−0.624	
					−0.658	−0.709		
					−0.676	−0.631		
O2 (0.5053, 0.3034, 0.5931)	−0.811	−0.642	−0.568	−0.587	−0.536	−0.709	−0.590	−0.541
				−0.681	−0.658	−0.705	−0.657	
					−0.691	−0.475		
					−0.676	−0.631		
O3 (0.5931, 0.5053, 0.3034)	−0.811	−0.642	−0.603	−0.581	−0.658	−0.475	−0.658	−0.682
				−0.641	−0.691	−0.709	−0.634	
					−0.536	−0.705		
					−0.676	−0.631		

[a] Atoms are identified by their fractional coordinates;[25] charges in columns 3−9 were scaled based on the factors obtained from converting bulk (unscaled) to the values from the chlorate potential[15] (bulk scaled); the unscaled surface and isolated charges can be derived by reversing this process; rows that contain more than one value indicate the possiblilty of considering a number of surface molecules.

using a classical attachment energy model. Therefore the polar nature of the crystal is not reproduced.

Polar Morphology Simulation using a Surface-Specific Attachment Energy Model. Two polar calculations were attempted. For the first model, the charges for the ions attaching to the growing crystal surfaces were taken to be different from those of the bulk crystal structure.[32] The calculated bulk charges (Table 4, column 2) were scaled to agree with the atomic charges given with the potential parameters (Table 4, column 3). The scaling factors used for each atom were then applied to the results for an isolated molecule to obtain the values to be assigned to the oncoming ions (Table 4, column 4). The attachment energies obtained from this calculation are detailed in Table 3, column 3, with the resultant morphology shown in Figure 6b. In this case, the polar nature of the crystal is still not predicted, because the growth rate along {111} is again calculated to be equal to that of {−1 −1 −1}. The morphology is virtually identical to that obtained via the classical attachment energy approach. Therefore, the use of bulk/isolated charge sets is insufficient to simulate the slower growth rate of the {−1 −1 −1} form.

For the second polar simulation, surface charges were assigned to the relevant surfaces (Table 4, columns 5−9), with the oncoming molecules again considered to have the charges of the isolated molecule. When more than one symmetry-independent molecule was observed at the surface under investigation, it was not clear which would give the optimum surface charge distribution, therefore, separate calculations were run for each individual molecule, with the average E_{att} value used. The attachment energies are tabulated in column 4 of Table 3. It is now apparent that the predicted growth rates of the {111} and {−1 −1 −1} forms are different, with the {−1 −1 −1} form having the smaller attachment energy and thus the lower growth rate. This result would indicate that the {−1 −1 −1} form will appear more dominant in the morphology than the {111} form. The morphology computed from these results bears out this prediction (see Figure 6c). As with the classical prediction, the {200} form is greatly underestimated, however the polar nature can be seen quite distinctly. This predicted morphology is apparently at variance with that detailed in refs 41 and 42, in which the {111} form is observed to be the dominant polar face. Our study relates to a published structure[16] that does not state its handedness; that is, there is no indication whether we are looking at the right-handed or left-handed form of the crystal form. Therefore, it is not possible to know which enantiomorph is considered − one would exhibit the {111} form and one the {−1 −1 −1}. In addition, a number of the experimental studies already discussed arbitrarily assign the {−1 −1 −1} form and so can be misleading. In the absence of information on the handedness of the crystals studied, these results are not in any conflict.

Rationalization of Predicted versus Experimental Data. A visualization of the chlorate packing structure can be used to help indicate if the chlorate growth may be affected by solvent or inhibited by additives on the habit faces {100}, {110}, {111} and {120}. Considering each face in turn (Figures 7a−c), we can start to allude to the possible interactions that could take place (the {120} form will not be discussed because its appearance is more rare).

For the {100} surface (Figure 7a), oxygens protrude from the surface, providing a possible site for hydrogen-bonding interactions with, for example, water molecules. This structure could be an indication of why the crystal grows with predominant {100} from aqueous solution. The water molecules attach to the surface and then desolvate slower than the other faces considered, thereby slowing the growth of the {100} surfaces, which therefore dominate the overall form. This result would indicate that the kinetics of desolvation are the rate-limiting step.

The {110} surface (Figure 7b) is a mixed surface of sodium cations and protruding oxygens. The surface is very crowded and is unlikely to have any substantial interaction with solvent molecules.

The {111} surface (Figure 7c) exhibits a cation (sodium)-rich environment that is likely to be susceptible to interaction with negative species of interaction molecules. Its Freidel opposite, the {−1 −1 −1} surface (Figure 7c) is not an equivalent surface because of the noncentrosymmetric nature of the structure. Termination of the bulk is mixed rather than predominately cationic. One out of four of the chlorate molecules is aligned with the chlorine atom toward the surface.

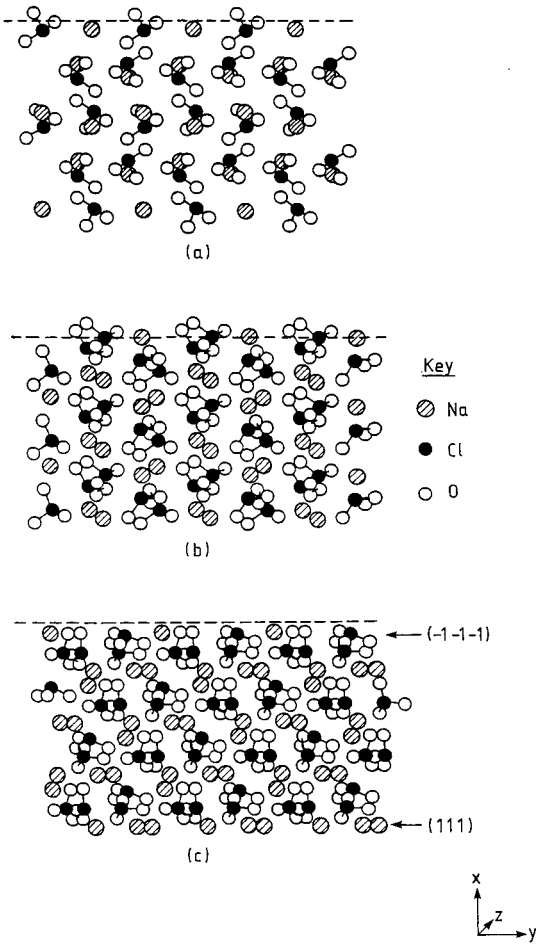

Figure 7. Surface visualization of the molecular arrangement on the habit surfaces of sodium chlorate: (a) {100}; (b) {110}; (c) {111} and $\{-1\ -1\ -1\}$.

This arrangement has been found to be important in defining the mechanism by which the additive, sodium dithionate, interacts with sodium chlorate.[41,42]

Conclusions

Using a combination of attachment energy and quantum chemical calculations, with the latter involving the use of full periodic boundary conditions, the prediction of the polar morphology of sodium chlorate has been carried out. The simulation is in reasonable agreement with observed morphologies, although there is an underestimation of the dominant {200} form. The latter is rationalized with experimental data via preferential solvent binding on these faces. The absolute polarity of the crystal with respect to the root structural data reveals the chlorate-rich $\{-1\ -1\ -1\}$ form is observed rather than the Freidel opposite {111} form.

Acknowledgment. The authors would like to thank E. I. du Pont de Nemours & Company for the provision of a Ph.D. studentship (G.B.T.), the EPSRC for the provision of research grants (GR/H/40891, GR/H/71994, GR/J/31834, GR/K/63160), postdoctoral research fellowships (P.J.W. and G.C.), and a Senior Fellowship (K.J.R.).

References and Notes

(1) Hartman, P.; Perdok, W. G. *Acta Crystallogr.* **1955**, *8*, 49.
(2) Lui, X. Y.; Bennema, P. *Phys. Rev. B: Condens. Matter* **1996**, *53*, 2314.
(3) Rohl, A. L.; Gay, D. H. *Min. Magn.* **1995**, *59*, 607.
(4) Myerson, A. S.; Saska, M. *ACS Symp. Ser.* **1990**, *438*, 55.
(5) Saska, M.; Myerson, A. S. *J. Cryst. Growth* **1983**, *61*, 546.
(6) Strom, C. S.; Bennema, P. *J. Cryst. Growth* **1997**, *173*, 150.
(7) Pfefer, G.; Boistelle, R. *Chem. Eng. Res. Des.* **1996**, *74*, 744.
(8) Bravais, M. A. *Études Crystallographiques*; Gauthier-Villars: Paris; 1866.
(9) Freidel, G. *Bull. Soc. Franç. Mineral.* **1907**, *30*, 326.
(10) Donnay, J. D. H.; Harker, D. *Am. Miner.* **1937**, *22*, 446.
(11) Hartman, P.; Bennema, P. *J. Cryst. Growth* **1980**, *49*, 145.
(12) Roberts, K. J.; Docherty, R.; Bennema, P.; Jetten L. A. M. J. *J. Phys. D: Appl. Phys.* **1993**, *26*, 7.
(13) Roberts, K. J.; Telfer, G. B.; Jackson, R. A.; Wilde, P. J.; Meenan, P. *J. Chem. Soc., Faraday Trans.* **1995**, *91*, 4133; see also, Green, D. A., Harlow, R. L., Meenan, P., Robertson, D. C., Telfer, G. B., Roberts, K. J., Jackson, R. A.; Wilde, P. J. *The 5th World Congress of Chemical Engineering, San Diego, California*, **1996**, *5*, 692.
(14) Telfer, G. B.; Wilde, P. J.; Jackson, R. A.; Meenan, P.; Roberts, K. J. *Philos. Mag. B*, **1996**, *73*, 147.
(15) Telfer, G. B.; Gale, J. D.; Roberts, K. J.; Jackson, R. A.; Wilde, P. J.; Meenan, P. *Acta Crystallogr.* **1997**, *A53*, 415; see also, Telfer, G. B. Ph.D. Thesis, University of Strathclyde, 1997.
(16) Burke-Laing, M. E.; Trueblood, K. N. *Acta Crystallogr.* **1977**, *B33*, 2698.
(17) Viwanathany, R. *J. Appl. Phys.* **1966**, *37*, 884.
(18) Bunn, C. *Chemical Crystallography*; Clarendon: Oxford, UK, 1961; p 21.
(19) Wojciechowski, K. Ph.D. Thesis, 1989, University of Strathclyde, UK.
(20) Kern, R. *Bull. Soc. Franc. Miner. Crist.* **1955**, *78*, 497.
(21) Simon, B. *J. Cryst. Growth* **1983**, *61*, 167.
(22) Hooper, R. M.; Roberts, K. J.; Sherwood, J. N. *J. Mater. Sci.* **1982**, *18*, 81.
(23) Ramachandran, G. N.; Chandrasekaran, K. S. *Acta Crystallogr.* **1957**, *10*, 671.
(24) Abrahams, S. C.; Bernstein, J. L. *Acta Crystallogr.* **1977**, *B33*, 3601.
(25) Szurgot, J.; Szurgot, M. *Cryst. Res. Technol.* **1995**, *30*, 71.
(26) Clydesdale, G.; Roberts, K. J.; Docherty, R. (a) *J. Cryst. Growth* **1996**, *166*, 78. (b) *Proc. Third International Workshop on the Crystal Growth of Organic Materials*, Washington D.C., *ACS Conference Proceedings Series*; Myerson, A.; Greeen, D. A.; Meenan, P., Eds.; 1996, p 43. (c) *QCPE Bull.* **1996**, *16(3)*, 1.
(27) CERIUS^2 molecular modelling software for materials research from Molecular Simulations Inc. of San Diego, CA and Cambridge, UK.
(28) Clydesdale, G.; Roberts, K. J.; Docherty, R. In *Controlled Particle, Droplet and Bubble Formation*; Wedlock, D., Ed.; Butterworth-Heinemann: London, 1994; p 119.
(29) Meenan, P. Ph.D. Thesis, University of Strathclyde, Glasgow, UK., 1992.
(30) Evjen, H. M. *Phys. Rev.* **1932**, *39*, 675.
(31) Davey, R. J.; Milisavljevic, B.; Bourne, J. R. *J. Phys. Chem.* **1988**, *92*, 2032.
(32) Docherty, R.; Roberts, K. J.; Saunders: V. R.; Black, S. N.; Davey, R. J. *Faraday Discuss.* **1993**, *95*, 11.
(33) Wireko, F. C.; Shimon, L. J.; Frolow, F.; Berkovitch-Yellin, Z.; Lehav, M.; Leiserowitz, L. *J. Phys. Chem.* **1987**, *91*, 472.
(34) Dovesi, R.; Saunders: V. R.; Roetti, C. CRYSTAL92 − An ab initio Hartree−Fock LCAO Program for Periodic Systems, 1992.
(35) Pisani, C.; Dovesi, R.; Roetti, C. *Hartree−Fock ab initio Treatment of Crystalline Systems*, Lecture Notes in Chemistry; Springer-Verlag: Heidelberg, 1988; Vol. 48.
(36) Pisani, C.; Dovesi, R. *Int. J. Quantum Chem.* **1980**, *17*, 501.
(37) Saunders: V. R. *Faraday Symp. Chem. Soc.* **1984**, *19*, 79.
(38) Dovesi, S.; Causa, M.; Orlando, R.; Roetti, C.; Saunders: V. R. *J. Chem. Phys.* **1990**, *92*, 7402.
(39) Saunders: V. R.; Freyria-Fava, C.; Dovesi, R.; Salasco, L.; Roetti, C. *Mol. Phys.* **1992**, *77*, 629.
(40) *CRC Handbook of Chemistry and Physics*, 77th ed. (1996−1997), CRC: New York, 1996; p 1221.
(41) Ristic, R.; Sherwood, J. N.; Wojciechowski K. *J. Phys. Chem.* **1993**, *97*, 10774.
(42) Ristic R.; Shekunov, B. Yu.; Sherwood, J. N. *J. Cryst. Growth* **1994**, *139*, 336.